Supporting information

Strong magneto-optical response of non-magnetic organic materials coupled to plasmonic nanostructures

Dzmitry Melnikau[1,2], Alexander A. Govyadinov[1*], Ana Sánchez-Iglesias[3], Marek Grzelczak[3,6], Luis M. Liz-Marzán[3,6,7], Yury P. Rakovich[4,5,6].*

[1]CIC NanoGUNE, Ave. Tolosa 76, 20018 Donostia-San Sebastian, Spain

[2]National University of Ireland Galway, University Road, Galway, Ireland

[3]CIC biomaGune, Paseo de Miramón 182, 20014 Donostia-San Sebastian, Spain

[4]Centro de Física de Materiales (MPC, CSIC-UPV/EHU) Paseo Manuel de Lardizabal 5, Donostia-San Sebastian, 20018, Spain

[5]Donostia International Physics Center (DIPC), Paseo Manuel de Lardizabal 4, Donostia-San Sebastian, 20018, Spain

[6]IKERBASQUE, Basque Foundation for Science, Maria Diaz de Haro 3, 48013, Bilbao, Spain

[7]Biomedical Research Networking Center in Bioengineering Biomaterials and Nanomedicine, Ciber-BBN, Paseo de Miramón 182, 20014 Donostia-San Sebastián, Spain

METHODS.

Chemicals. Cyanine dyes 5,5′,6,6′-Tetrachloro-1,1′,3,3′-tetraethyl-imidacarbocyanine iodide (JC1), tetrachloroauric acid ($HAuCl_4$), sodium borohydride ($NaBH_4$), hexadecyltrimethylammonium bromide (CTAB), benzyldimethylhexadecylammonium chloride (BDAC), silver nitrate ($AgNO_3$), hydrochloric acid (HCl), ascorbic acid (AA) were purchased from Sigma-Aldrich. Cyanine dye 5,6-Dichloro-2-[[5,6-dichloro-1-ethyl-3-(4-sulfobutyl)-benzimidazol-2-ylidene]-propenyl]-1-ethyl-3-(4-sulfobutyl)-benzimidazolium hydroxide, inner salt, sodium salt S0046 (S-46) were obtained from FEW Chemicals.

Synthesis of gold nanorods. Gold nanorods were prepared using Ag-assisted seeded growth.[1] Seeds were prepared by the reduction of $HAuCl_4$ (5 mL, 0.25 mM) with $NaBH_4$ (0.3 mL, 10 mM) in aqueous CTAB solution (100 mM). An aliquot of seed solution (0.12 mL) was added to a growth solution containing CTAB (50 mL, 100 mM), $HAuCl_4$ (0.5 mL, 50 mM), ascorbic acid (0.4 mL, 100 mM), $AgNO_3$ (0.6 mL, 10 mM) and HCl (0.95 mL, 1000 mM). The mixture was left undisturbed at 30 ºC for 2 h. The solution was centrifuged twice (8000 rpm, 30 min) and redispersed in BDAC (10 mM) to obtain a final concentration of gold equal to 0.25 mM. The maximum of LSPR of initial gold nanorods was 860 nm.

Synthesis of Au@Ag core-shell nanorods. Core-shell Au@Ag nanorods were synthesized using benzyldimethylhexadecylammonium chloride (BDAC) as the capping.[2] The typical reaction involved the addition of different amount of $AgNO_3$ (10 mM) and ascorbic acid (100 mM) to the solution of gold nanorods (10 mL, 0.25 mM) at 60 ºC. Larger amount of silver caused more pronounced blue shift of the LSPR. To reach the maximum of LSPR at 609, 636, 668, 695, 712, 794, 826 nm was added 1.0, 0.9, 0.8, 0.6, 0.4, 0.25, 0.13 mL of $AgNO_3$ (10 mM) while maintaining the molar ratio of Ascorbic Acid to Ag^+ equal to 4. The solutions were left for 3 hours at 60 ºC under magnetic stirring. Finally, the solutions were centrifuged twice (6000-9000 rpm, 40 min) and redispersed in BDAC (2 mL, 15 mM).

Preparation of J-aggregates. J-aggregates of the JC1 dye form spontaneously upon dissolution of this dye in water at pH8,[3, 4] while the formation of J-aggregates of another cyanine S-46 dye required the addition of polyelectrolyte: poly(diallyldimethylammonium chloride (PDDA) or polyethyleneimine (PEI).

Preparation of hybrid core-shell Au@Ag nanorods and J-aggregates system. The production of the hybrid Au@Ag nanorods and J-aggregates system relies upon the electrostatic

interactions between the anionic groups of the J-aggregates and the cationic sites of stabilizing agent BDAC at the surface of bare Au@Ag nanorods. Hybrid structures of core-shell Au@Ag nanorods and J-aggregates were produced by addition of 10 µl of concentrated ethanol solution of JC1 dye to 1 ml of an aqueous solution of core-shell Au@Ag nanorods in the presence of ammonia (pH=8), followed by gentle stirring for 15 minutes. In order to separate J-aggregates, which bound to nanorods, from monomer dye molecules and free J-aggregates the solution was centrifuged at 4000 rpm for 5 minutes and re-dispersed in water.[4, 5]

Instrumentation. The optical extinction spectra were measured using a Cary 50 spectrometer (Agilent Technologies).

A transmission electron microscopy (TEM) image of nanorods obtained using transmission electron microscope FEG-TEM of type JEOL JEM-2100F UHR.

For the magnetic circular dichroism (MCD) measurements we used Jasco J-815 spectropolarimeter equipped with a water cooled GMW 3470 electromagnet providing a static magnetic field of up to 1 T. The total magnetic circular dichroism was calculated as $\Delta A_0 = \theta / \left(\frac{\ln 10}{4}\right)$, where θ is the measured ellipticity. ΔA_0 is the sum of natural CD due to molecular symmetry and the MCD induced by the magnetic field. The natural CD was measured as the signal at zero magnetic field, B, and then subtracted from ΔA_0, yielding the MCD (ΔA) – the difference in absorbance between the right and the left hand polarized light induced by an external magnetic field.[6] ΔA depends of the absorbent concentration and can be written as: $\Delta A = \Delta\varepsilon_M clB$,[7] where l is the path length through the sample, c is the molar concentration and $\Delta\varepsilon_M$ is the differential molar extinction. For proper comparison of MCD between samples of different concentration we normalize the MCD on the absorption maximum $A_{\max}$ according to $\Delta A(\lambda)/(A_{\max} B) \propto \Delta\varepsilon_M$, where $A_{\max}$ is the absorption maximum for the particular sample. Such normalization essentially yields the intrinsic MCD parameter $\Delta\varepsilon_M$. Another representation is the normalization of MCD on the absorption spectra $A(\lambda)$ according to $\Delta A(\lambda)/(A(\lambda)B) = \Delta\varepsilon_M(\lambda)/\varepsilon(\lambda)$, where $\varepsilon(\lambda)$ is molar extinction coefficient spectra. Such normalization shows the relative enhancement of MO activity with respect to the pure light extinction.

In this work we regard the extinction spectra measured by our spectrometer as absorption spectra due to weak scattering in our samples.

All absorption and MCD spectra were measured in aqueous solutions (using doubly purified deionized water from an 18 MU Millipore system) and identical 2mm long quartz cuvette. All experiments were performed in an ambient atmosphere at room temperature.

Calculations of the absorption and MCD for a nanorods solution. The dielectric response of a nanorod solution could be described by the effective tensor of dielectric permittivity $\bar{\bar{\epsilon}}_{\text{eff}}$. To determine its components we model the rods as prolate spheroidal particles composed of three concentric shells with major semiaxes a_m and minor semiaxes $b_m = \nu a_m$, where ν is the aspect ratio (same for all shells). The polarization $\vec{P}$ of such a particle is the sum of the polarizations in each shell

$$\vec{P} = \sum_{m=1}^{3} t_m \vec{P}_m = \sum_{m=1}^{3} t_m (\bar{\bar{\epsilon}}_m - \bar{\bar{\epsilon}}_h)\vec{F}_m \qquad (1)$$

where $\vec{F}_m$ is the homogeneous electric field in the m-th shell, t_m is the shell's volume fraction with respect to the total particle volume, $\bar{\bar{\epsilon}}_m$ is its tensor of dielectric permittivity of the shell material and $\bar{\bar{\epsilon}}_h$ is that of host medium which surrounds the particle. The total electric flux density can then be written as

$$\vec{D} = \bar{\bar{\epsilon}}_h \vec{E} + f\vec{P} \equiv \bar{\bar{\epsilon}}_{\text{eff}} \vec{E} \qquad (2)$$

where $\vec{E} = (1-f)\vec{F}_0 + f\sum_{m=1}^{3} t_m \vec{F}_m$ is the average electric field existing in the solution with volume concentration of particles, f and $\bar{\bar{\epsilon}}_h = \epsilon_h \hat{1}$ is the permittivity of host medium ($\hat{1}$ is the identity matrix). By iteratively relating electric fields in subsequent shells to their neighbors through boundary conditions, one can express $\vec{F}_m$ through the field in the host $\vec{F}_m = \bar{\bar{S}}_m \vec{F}_0$, where $\bar{\bar{S}}_m$ is a the matrix given in ref.[8] Thus if the tensorial permittivities for all particle shells are known, one can solve Eq. (2) and find $\bar{\bar{\epsilon}}_{\text{eff}}$.

With a uniform external magnetic field B directed, for example, along z-axis, the permittivity tensors of metallic shells can be written in the form:

$$\bar{\bar{\epsilon}}_{2,3} = \begin{pmatrix} \epsilon & iA & 0 \\ -iA & \epsilon & 0 \\ 0 & 0 & \epsilon \end{pmatrix} \qquad (3)$$

Where $\epsilon = \epsilon(\omega)$ is the bulk dielectric function of the considered metal and $A \propto B$ is the anisotropic response due to magnetic field. In the following we employ Drude model to describe the permittivities of Au and Ag, i.e.

$$\epsilon(\omega) = \epsilon_\infty - \frac{\omega_p^2}{\omega^2 + i\gamma\omega} \quad (4)$$

where ω_p is the metal plasma frequency, γ is the electron collision rate and ϵ_∞ is the high-frequency component of the permittivity. For silver we use $\omega_p = 9.1$ eV and $\epsilon_\infty = 5.3$, which accounts for the interzone transitions.[9] For gold we use ω_p =8.67 eV and model the contribution from the intraband transition according to the model of Ref.[10] The collision rates were fitted to the widths of the experimental absorption peaks of pure Au/Ag solutions, which in our experiment is dominated by the inhomogeneous broadening due to natural nanorod size dispersion. The corresponding values are $\gamma = 0.27$ eV and 0.3 eV for Ag and Au, respectively.

The off-diagonal component A can be further written as[8, 11]

$$\mathrm{A}(\omega) = -\frac{\omega_p^2 \omega_\mathrm{c}}{\omega {\gamma_\infty}^2}\left(1 - \frac{i\omega}{\gamma_\infty}\right)^2 \quad (5)$$

where $\omega_c = Be/m_e$ is the cyclotron frequency (e and m_e are the electron charge and mass).

The intrinsic magnetootical response of the J-aggregates is assumed to be negligible yielding purely diagonal form of permittivity tensor $\bar{\bar{\epsilon}}_1 = \epsilon_\mathrm{J}\hat{1}$ with ϵ_J described by a simple Lorentzian:

$$\varepsilon_J(\omega) = \epsilon_0 + f_J \frac{\omega_0^2}{\omega_0^2 - \omega^2 - i\gamma_J\omega} \quad (6)$$

with parameters $\epsilon_0 = \epsilon_\mathrm{h}$, f_J = 0.06, and γ= 0.036, ω_0=2.13 eV similar to those used in Ref.[12, 13]

It can be verified that the effective permittivity tensor retains the same form as its constituents $\bar{\bar{\epsilon}}_1$ and $\bar{\bar{\epsilon}}_2$, i.e.:

$$\bar{\bar{\epsilon}}_\mathrm{eff} = \begin{pmatrix} \epsilon_x & iA_e & 0 \\ -iA_e & \epsilon_y & 0 \\ 0 & 0 & \epsilon_z \end{pmatrix}$$

with (in general) non-identical diagonal components. The response of the solution with random particle orientation can be calculated as an average of $\bar{\bar{\epsilon}}_\mathrm{eff}$ for $B||x$, $B||y$ and $B||z$, yielding the effective permittivity tensor in the form: $\langle\bar{\bar{\epsilon}}_\mathrm{eff}\rangle = \epsilon_\mathrm{eff}\hat{1} + A_\mathrm{eff}\,\hat{\sigma}$, where $\hat{1}$ is the identity matrix and

$$\hat{\sigma} = \begin{pmatrix} 0 & i & 0 \\ -i & 0 & 0 \\ 0 & 0 & 0 \end{pmatrix}$$

The optical absorption experienced by a plane wave can then be calculated by[14]

$$A = \Im\left(\sqrt{\epsilon_{\text{eff}}}\right)$$

The corresponding MCD signal is[11]

$$\Delta A = \frac{1}{2}\Im\left(\sqrt{\epsilon_{\text{eff}} + A_{\text{eff}}} - \sqrt{\epsilon_{\text{eff}} - A_{\text{eff}}}\right)$$

In our calculations, we fixed the short and the long semiaxes of the Au core for all samples at 6 nm and 30 nm, respectively. These values were obtained from the TEM images presented in Fig. 1c of the main text, which show a darker contrast for the nanorod cores. The aspect ratios of the Ag shell for each sample were fitted to reproduce the experimental extinction spectra of bare NRs systems. J-aggregates were assumed to form a uniform shell of thickness $d \approx 3$ nm. The host was assumed to be water with the dielectric permittivity of ϵ_{h}=1.33[2].

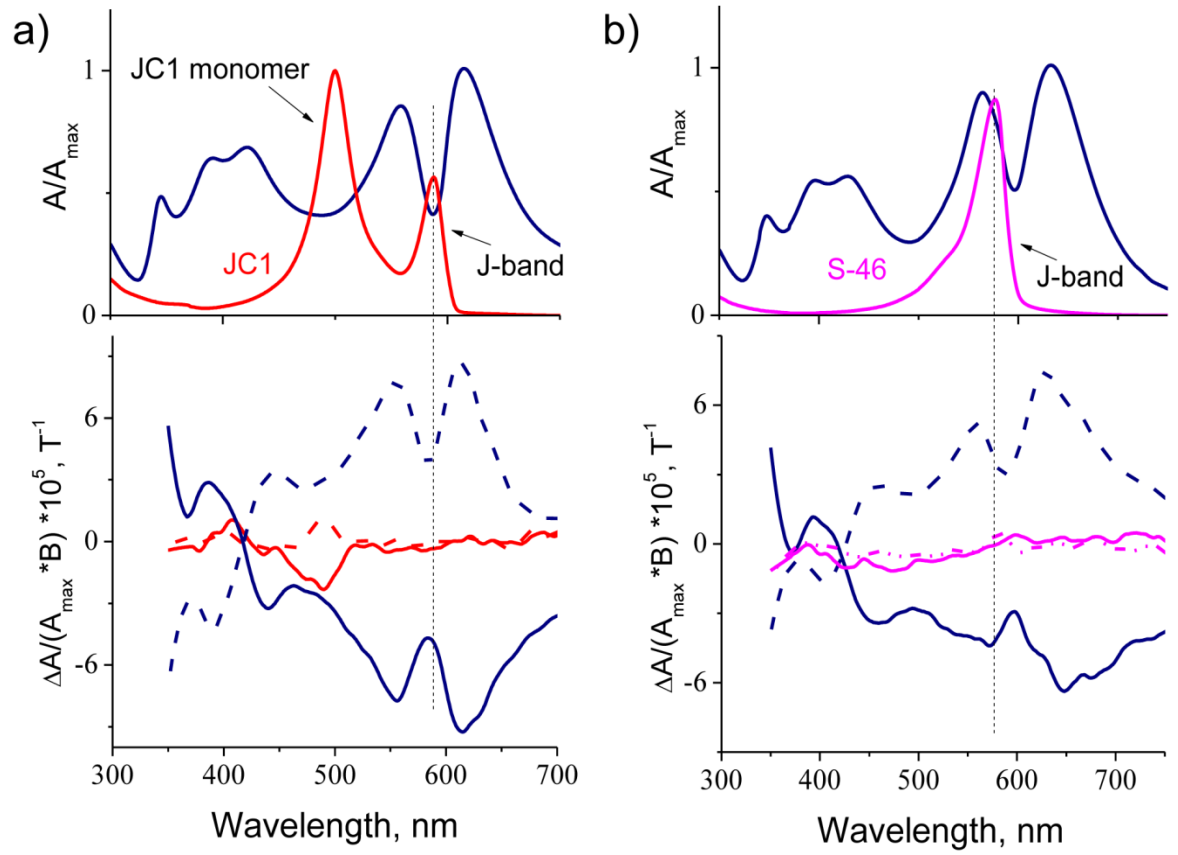

Figure S1: Experimental extinction (top) and magnetic circular dichroism spectra (down) of (a) the hybrid core-shell Au@Ag nanorods and J-aggregates cyanine dye JC1 system (blue line) and pure JC1 J-aggregates (red line); and (b) hybrid core-shell Au@Ag nanorods and J-aggregates cyanine dye S-46 system (blue line) and pure S-46 J-aggregates (purple line). MCD spectra were obtained under the magnetic fields B= 1T (solid lines) and B= -1T (dashed lines). Note that we registered the negligible MCD for J-aggregates of both JC1 and S-46 dyes. Small MCD signal for the JC1 monomer is irrelevant for this study due to its absence in the samples after purification as described in text.

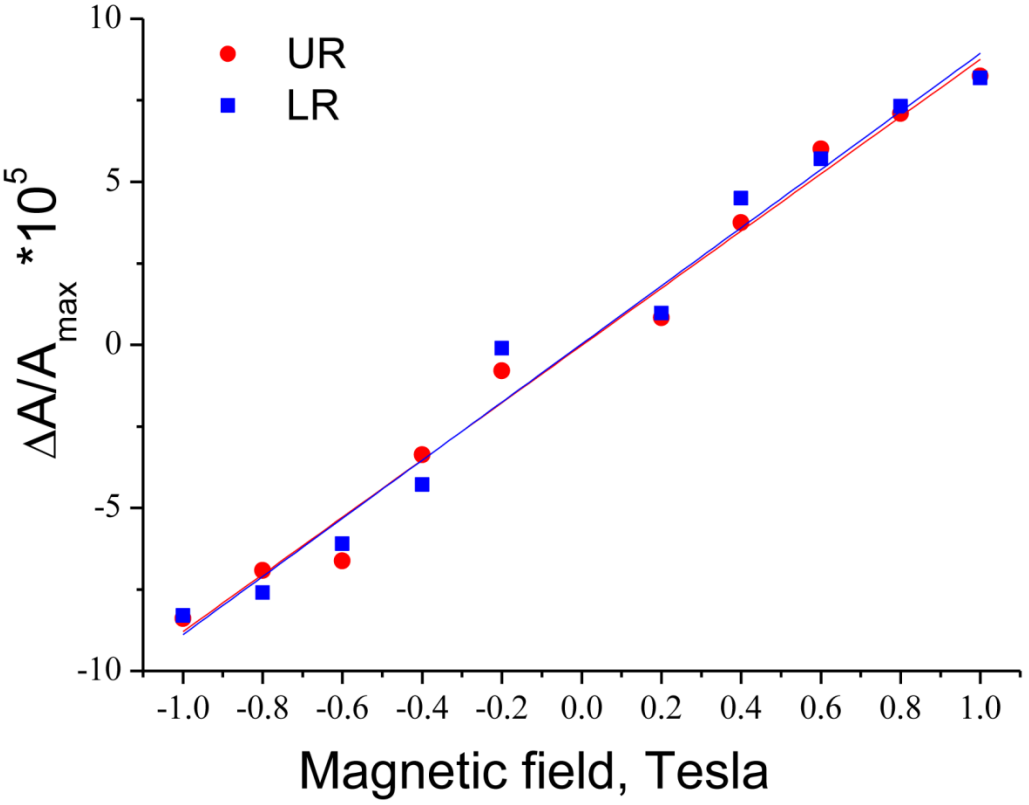

Figure S2. Dependence of the MCD on the value of the magnetic field at UR (red circles) and LR (blue squares) of hybrid core-shell Au@Ag and J-aggregates system with nanorod aspect ratio of 2.5 (resonance conditions). The MCD signal was normalized to the maxima of the UR and LR extinction peaks, respectively.

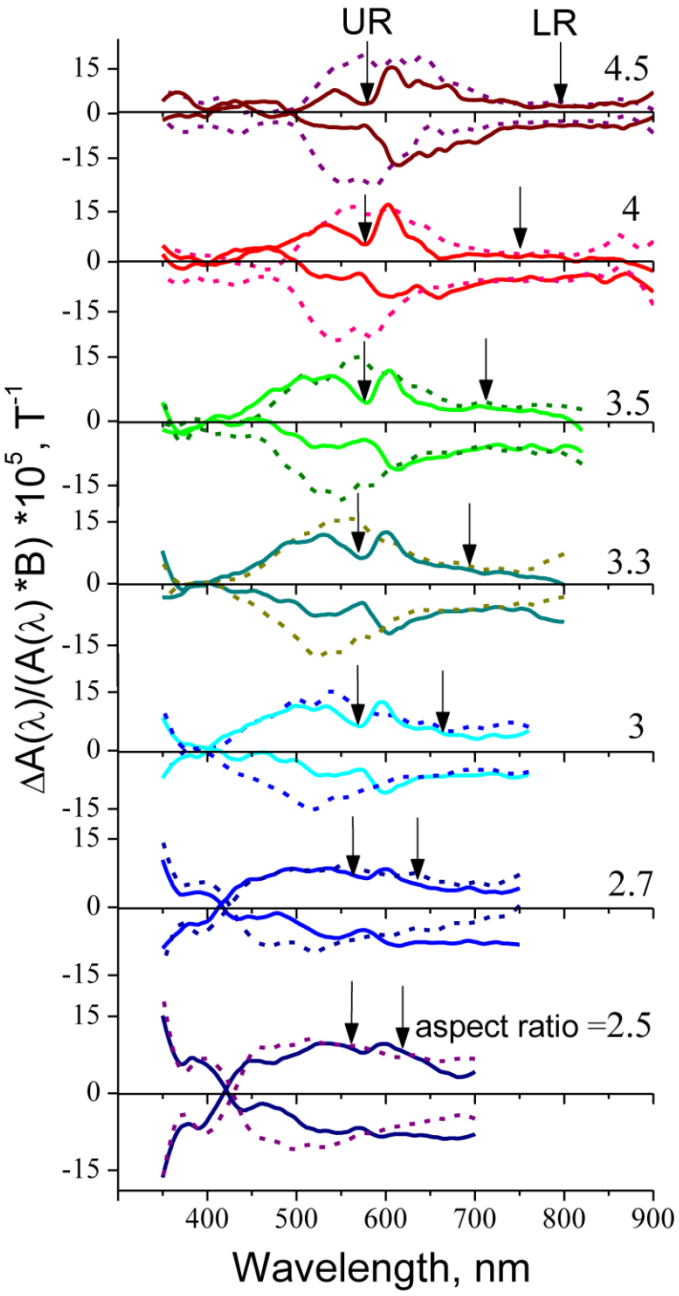

Figure S3. Experimental MCD spectra for bare core-shell Au@Ag nanorods (dotted lines) and for hybrid core-shell Au@Ag and J-aggregates system (solid lines) normalized to the corresponding absorption spectra and the magnetic field. The vertical black lines indicate the spectral positions of the UR and LR.

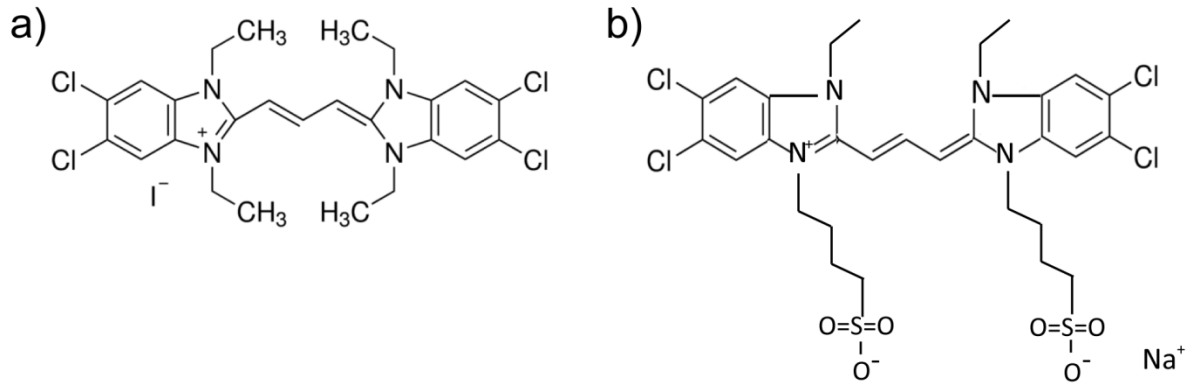

Figure S4: Chemical structures: (a) JC1 dye (5,5′,6,6′-Tetrachloro-1,1′,3,3′-tetraethyl-imidacarbocyanine iodide, 5,5′,6,6′-Tetrachloro-1,1′,3,3′-tetraethylbenzimidazolocarbocyanine iodide) (b) S-46 dye (5,6-Dichloro-2-[[5,6-dichloro-1-ethyl-3-(4-sulfobutyl)-benzimidazol-2-ylidene]-propenyl]-1-ethyl-3-(4-sulfobutyl)-benzimidazolium hydroxide, inner salt, sodium salt)

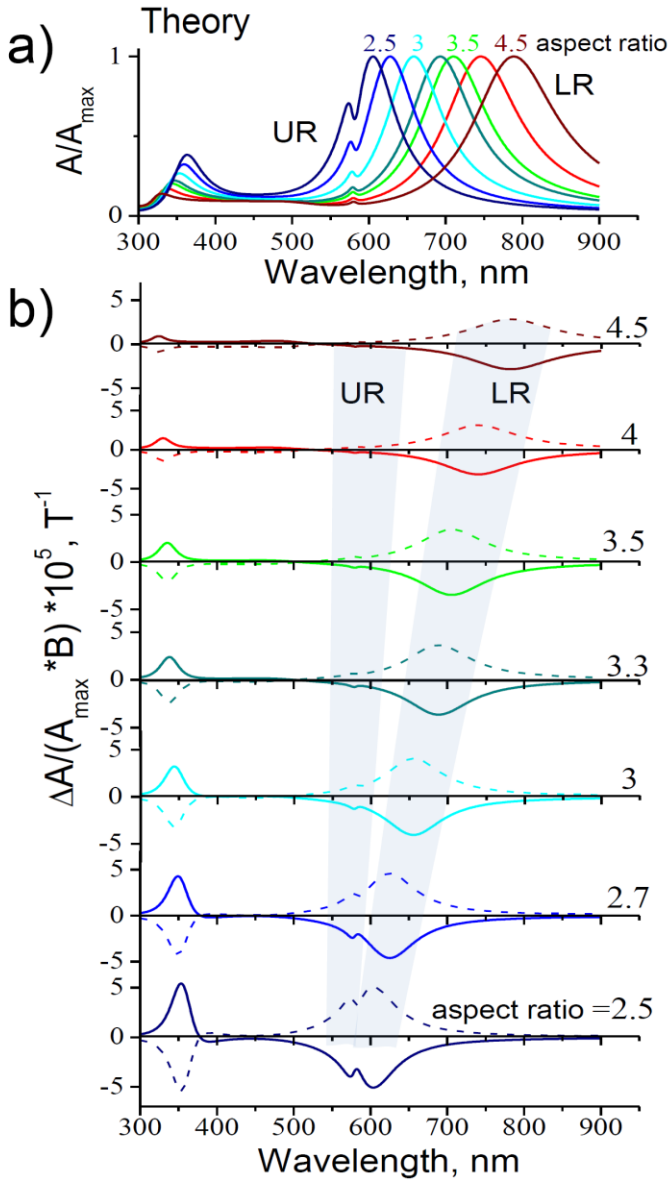

Figure S5. The theoretical extinction spectra (a) and MCD spectra (b) of the hybrid system of J-aggregates and core-shell Au@Ag nanorods for different aspect ratios, assuming five times smaller value of the dye oscillator strength (f_J=0.012) compared to the value that fits our experimental data. The corresponding coupling constant $g/\kappa = 0.27$ is only slightly above the strong coupling threshold, yet the MO activity of the upper plexciton is clearly seen (for small detunings). All spectra are normalized the same way as in Figure 3 of the main article. The solid and dashed lines correspond to B= $\pm$1T, respectively.

SUPPLEMENTAL REFERENCES

1. Liu, M. Z.; Guyot-Sionnest, P. *J Phys Chem B* **2005,** 109, (47), 22192-22200.

2. Gomez-Grana, S.; Goris, B.; Altantzis, T.; Fernandez-Lopez, C.; Carbo-Argibay, E.; Guerrero-Martinez, A.; Almora-Barrios, N.; Lopez, N.; Pastoriza-Santos, I.; Perez-Juste, J.; Bals, S.; Van Tendeloo, G.; Liz-Marzan, L. M. *J Phys Chem Lett* **2013,** 4, (13), 2209-2216.

3. Melnikau, D.; Savateeva, D.; Gun'ko, Y. K.; Rakovich, Y. P. *J. Phys. Chem. C* **2013,** 117, (26), 13708–13712.

4. Melnikau, D.; Savateeva, D.; Susha, A.; Rogach, A. L.; Rakovich, Y. P. *Nanoscale Res. Lett.* **2013,** 8.

5. Melnikau, D.; Esteban, R.; Savateeva, D.; -Iglesias, A. S.; Grzelczak, M.; Schmidt, M. K.; Liz-Marzan, L. M.; Aizpurua, J.; Rakovich, Y. P. *J. Phys. Chem. Lett.* **2016,** 7, (2), 354-362.

6. Sutherland, J. C.; Holmquist, B. *Annu Rev Biophys Bio* **1980,** 9, 293-326.

7. Mason, W. R., *A practical guide to magnetic circular dichroism spectroscopy*. Wiley-Interscience: Hoboken, N.J., 2007; p xii, 223 p.

8. Abe, M.; Suwa, T. *Phys. Rev. B* **2004,** 70, (23).

9. Palik, E. D.; Ghosh, G., *Handbook of optical constants of solids*. Academic Press: San Diego, 1998.

10. Etchegoin, P. G.; Le Ru, E. C.; Meyer, M. *J Chem Phys* **2007,** 127, (18).

11. Hui, P. M.; Stroud, D. *Appl. Phys. Lett.* **1987,** 50, (15), 950-952.

12. Yoshida, A.; Kometani, N. *J. Phys. Chem. C* **2010,** 114, (7), 2867–2872.

13. Fofang, N. T.; Park, T. H.; Neumann, O.; Mirin, N. A.; Nordlander, P.; Halas, N. J. *Nano Lett.* **2008,** 8, (10), 3481-3487.

14. Zvezdin, A. K.; Kotov, V. A., *Modern magnetooptics and magnetooptical materials*. Institute of Physics Pub.: Bristol Philadelphia, Pa., 1997; p xv, 386 p.